Effects of different wind deflectors on wind loads for extra-large cooling towers

S.T. Ke[*1,2], P. Zhu[3a] and Y.J. Ge[2b]

[1]*Department of Civil Engineering, Nanjing University of Aeronautics and Astronautics, Nanjing 210016, China*
[2]*State Key Laboratory for Disaster Reduction in Civil Engineering, Tongji University, Shanghai 200092, China*
[3]*Tower college, China Information Consulting & Designing Institute Co, LTD, Nanjing 210019, China*

Abstract. In order to examine the effects of different wind deflectors on the wind load distribution characteristics of extra-large cooling towers, a comparative study of the distribution characteristics of wind pressures on the surface of three large cooling towers with typical wind deflectors and one tower without wind deflector was conducted using wind tunnel tests. These characteristics include aerodynamic parameters such as mean wind pressures, fluctuating wind pressures, peak factors, correlation coefficients, extreme wind pressures, drag coefficients and vorticity distribution. Then distribution regularities of different wind deflectors on global and local wind pressure of extra-large cooling towers was extracted, and finally the fitting formula of extreme wind pressure of the cooling towers with different wind deflectors was provided. The results showed that the large eddy simulation (LES) method used in this article could be used to accurately simulate wind loads of such extra-large cooling towers. The three typical wind deflectors could effectively reduce the average wind pressure of the negative pressure extreme regions in the central part of the tower, and were also effective in reducing the root of the variance of the fluctuating wind pressure in the upper-middle part of the windward side of the tower, with the curved air deflector showing particularly. All the different wind deflectors effectively reduced the wind pressure extremes of the middle and lower regions of the windward side of the tower and of the negative pressure extremes region, with the best effect occurring in the curved wind deflector. After the wind deflectors were installed the drag coefficient values of each layer of the middle and lower parts of the tower were significantly higher than that without wind deflector, but the effect on the drag coefficients of layers above the throat was weak. The peak factors for the windward side, the side and leeward side of the extra-large cooling towers with different wind deflectors were set as 3.29, 3.41 and 3.50, respectively.

Keywords: extra-large cooling towers; wind deflector; fluctuating wind pressure; peak factor; pressure extremes; drag coefficient

1. Introduction

Great importance has been attached by researchers and designers to the wind safety performances of large hyperbolic cooling towers, an important structure in a thermal/nuclear power plant. Since the 1965 accident during which the three cooling towers in the Ferrybridge Power Station in Britain were destroyed by medium speed wind (Armitt 1980, Holmes 1992, Goudarzi *et al.* 2008, Ke *et al.* 2012, Ke e*t al.* 2013), scholars from both China and across the world have conducted in-depth research on the wind loads and wind effects on the towers (Davenport 1967, Isyumov *et al.* 1972, Bartoli *et al.* 1997, Sun *et al.* 1995, Zhao *et al.* 2016) and interference effects of the group towers (Sun *et al.*1992, Niemann *et al.* 1998, Harte *et al.* 2009, Qiao *et al.* 2011). Among them, Armitt (1980) has tried the wind tunnel test of the continuous medium pneumatic elastic model of cooling tower. The test results show that as the wind speed increases, the ripple wind
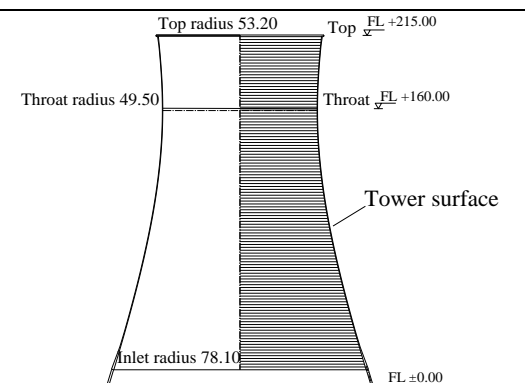
vibration effect of cooling tower is much higher than that of static wind effect, and its dynamic response cannot be ignored. Sun conducted the double-tower interference wind tunnel test with the rigid model, comprehensively analyzed the body coefficient of the two towers under various arrangement conditions, and divided the wind direction Angle into three regions according to the different influence degree. Sun *et al.* (1992) used the rigid model to carry out the wind tunnel test on the Twin Towers, and analyzed the figure coefficient of the two towers in all sorts of arrangement, and divided the wind direction into 3 regions according to the different degree of influence. Niemann *et al.* (1998) has carried out the wind tunnel test of the rigid model of the cooling tower to measure the quasi static pressure distribution on the surface of the cooling tower, and the response of the cooling tower to the fluctuating wind load is divided into the quasi static response and the resonance response. Relevant research has well supported the wind resistance design of large wind hyperbolic cooling towers. However, current studies not only fail to consider the impact of inlet wind deflectors on the cooling towers, but are also flawed with a lack of qualitative and quantitative research on the impact of different wind deflectors on the local and global wind load of cooling towers. Particularly at present, surface pressure extremes have become one of the control loads of the cooling tower structure design, so their values used in the design are directly related to the structural safety performance and the

*Corresponding author, Professor
E-mail: keshitang@163.com
[a] Engineer
E-mail: zhupeng2248@cicdi.com
[b] Professor
E-mail: yaojunge@tongji.edu.cn

Table 1 Size parameters of primary parts and structural schematic of the cooling tower

Part	Size	Schematic
Tower height	215.0 m	
Throat altitude	160.0 m	
Top radius	53.2 m	
Inlet radius	78.1 m	
Throat radius	49.5 m	
Thickness	0.26-1.30 m	
Columns	48 pairs of Λ	

(a) measuring point layout of cooling tower   (b) flow direction
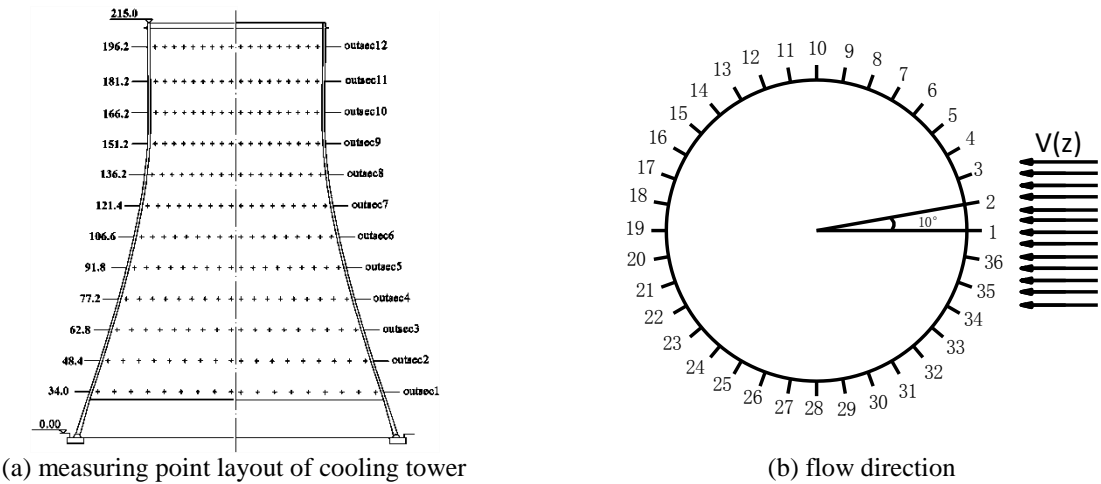
Fig. 1 Layout of cooling tower and angle of flow

(a) without air-deflecting   (b) external feed tank   (c) rectangular wind deflector   (d) curved wind deflector
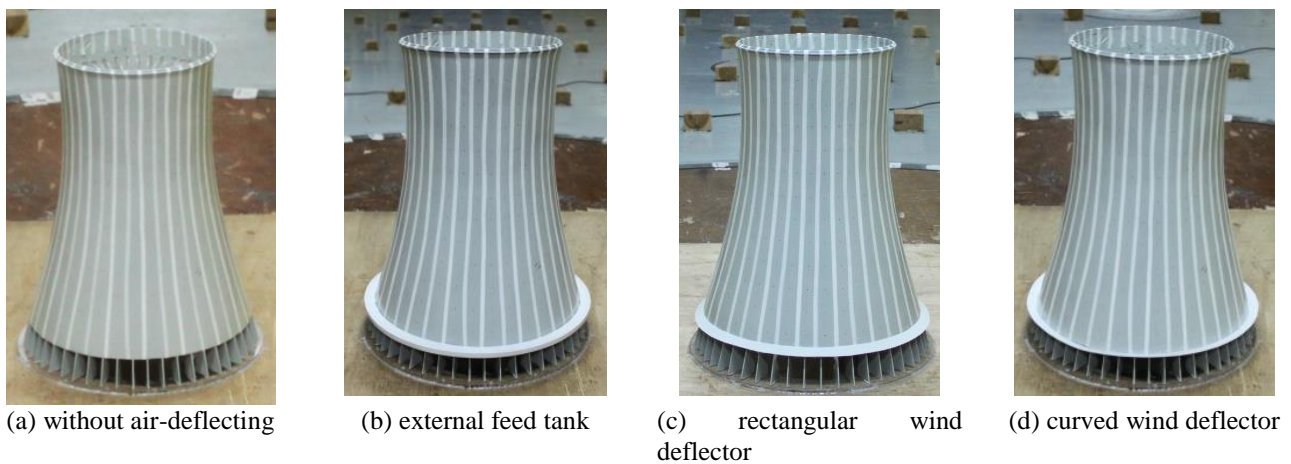
Fig. 2 The schematic view of cooling towers with different wind deflectors

overall construction cost of a cooling tower. Therefore, research on the characteristics of the average and extreme wind load distribution on the surface of cooling towers installed with different wind deflectors has important engineering implications.

In view of the above, this comparative study examined the impacts of three different wind deflectors which were added to an extra-large nuclear cooling tower (215 m high) in a Chinese power plant on the aerodynamic parameters, such as mean wind pressure, fluctuating wind pressure,
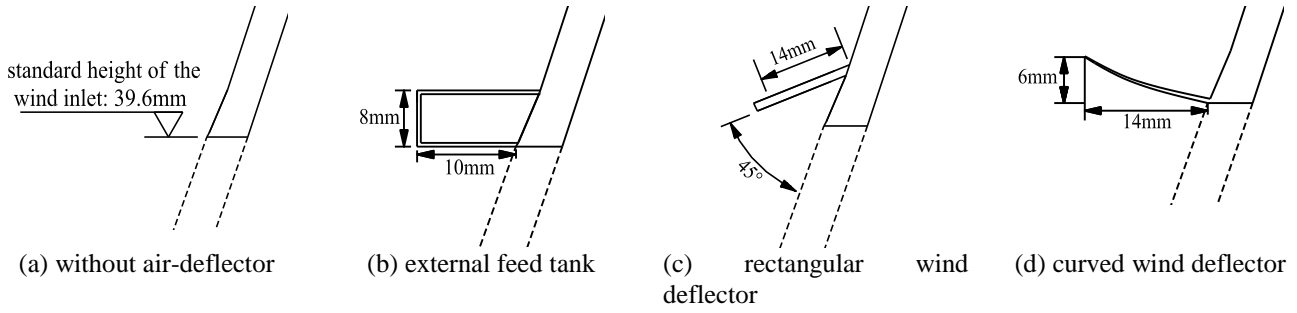
Fig. 3 Measurement details of different wind deflectors models

(a) comparison of test and the specified values

(b) comparison of fluctuating spectrum

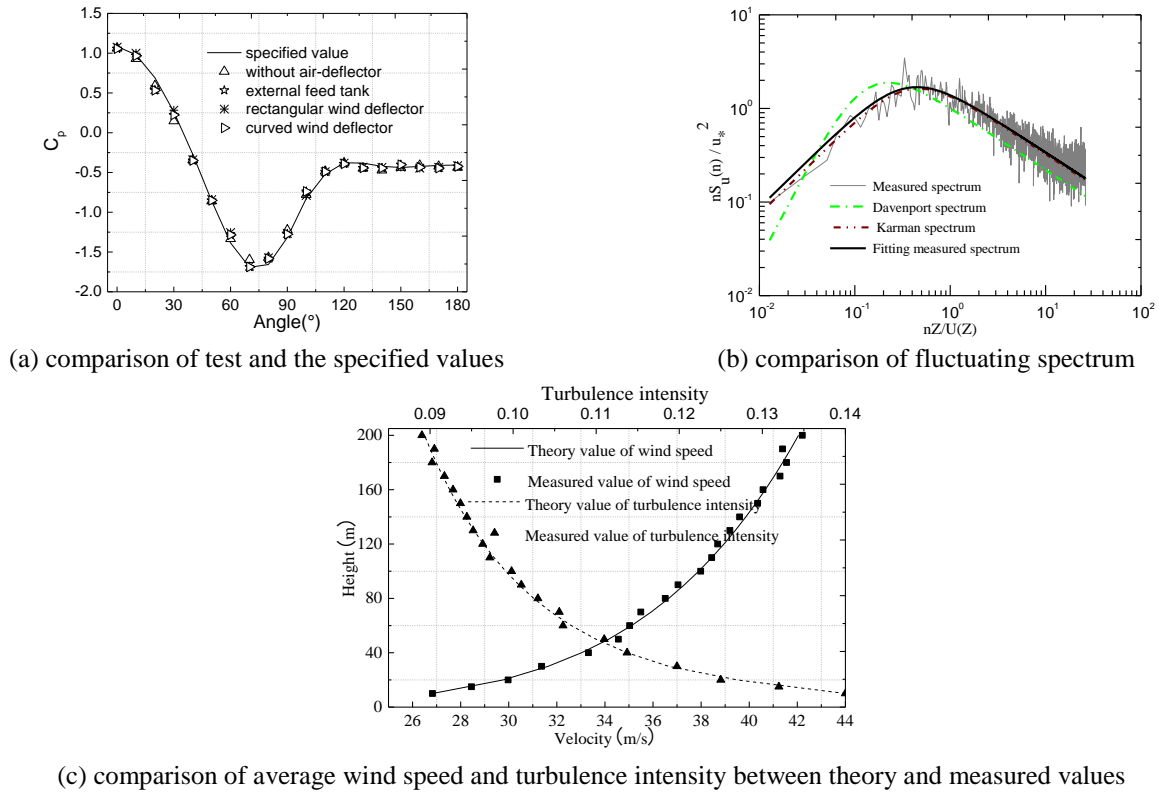(c) comparison of average wind speed and turbulence intensity between theory and measured values

Fig. 4 Comparison between the average wind pressure and wind field simulation schematic diagram

peak factor, correlation coefficient, pressure extreme, drag coefficient and vorticity distribution using wind tunnel tests. The pattern of impact of different wind deflectors on the global and local wind pressure distribution on the large cooling tower was extracted and the fitting formula of pressure extremes of the cooling tower with different wind deflectors was provided. The conclusions from this study can provide a scientific basis for setting the wind load values when designing wind deflectors for extra-large hyperbolic cooling towers.

2.3 Reynolds number effect simulation

The wind tunnel used in the rigid body pressure test of the cooling towers was a low speed closed reflux wind tunnel with a string of double test section and an all-steel structure. The main test section was 3 m wide, 2 m high and

20 m long. The wind speed was continuously adjustable, with the maximum wind speed up to 45 m/s; the pressure measurement system adopted was the electronic pressure scanner produced by Scanivalve. The triangular wedge and ground roughness elements were set in front of to the flow to simulate the atmospheric boundary layer of class B topography. Limited by the space and the subject, the paper will not provide the mean and the cross-sectional results of the turbulent wind obtained from the wind tunnel simulation.

The prototype structure of the large cooling tower has a range of Reynolds number of $1.5\times10^8 \sim 3.5\times10^8$ under the designed wind speed. Due to the limitations of the physical wind tunnel itself, it is difficult to reproduce the morphology of flow around the surface under such a high Reynolds number simply by increasing the wind speed in the test or enlarging the geometrical size of the structural model. The characteristics of the flow around cylinder-like structures have not only to do with the Reynolds number,

(a) divided the grid area
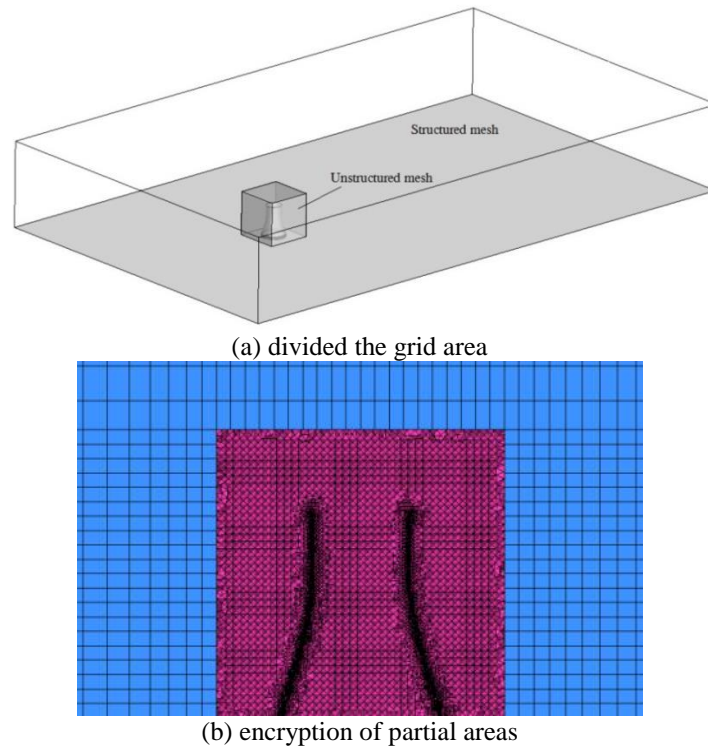

(b) encryption of partial areas

Fig. 5 The mesh diagram of cooling tower in the numerical simulation with partial encryption

but are also closely related to the surface roughness. Therefore, adjusting the surface roughness of the model can approximate the flow features under a high Reynolds number (Bartoli *et al*. 1997, Busch *et al*. 2002, Goudarzi *et al*. 2008, Zhao and Ge 2010).

A comparison of a variety of schemes to change the surface roughness led to the method of sticking rough tapes on the surface (a total of 36 rough paper tapes were stuck vertically and circumferentially, and evenly spaced with 5 mm in between and each tape was 0.1 mm thick,) and adjusting the test wind speed (10 m/s) to simulate high Reynolds number effects. The comparison shown in Fig. 4 indicates that the average surface pressure coefficient distribution of the middle cross-sections of the cooling tower agreed well with the specified values when the rough tapes were stuck on the surface and the test wind speed was at 10 m/s. In the entire study, this same roughness was adopted in the all cooling tower models with different wind deflectors.

2.4 Geometric modeling and mesh grid of CFD numerical simulation

In order for the flow to completely develop, the calculating domain was taken as 18D × 12D × 5D (flow direction × span-wise direction × vertical direction, D is the inlet diameter of cooling tower). The cooling tower was setup at a distance of 5D to the entry to ensure that the wake flow can fully develop. Due to the complexity of the shell and columns surface, hybrid mesh discrete mode was used and the complete calculating domain was divided into two parts, where the core region was meshed by tetrahedron and

local mesh around the cooling tower was encrypted, while the outer region was meshed by fine hexahedron mesh. The total number of mesh was 7.5 million. The calculating domain and details of meshing are shown in Fig. 5.

2.5 Boundary conditions and parameters setting

The boundary condition of the entry was defined as velocity entry in which the ground roughness coefficient of the wind velocity section was 0.15 type B geologic condition and the basic wind velocity at a reference height of 10 m was 26 m/s. The distribution form with respect to type B geologic conditions in China was used for the turbulence strength section. The boundary condition of inflow and FLUENT were connected by user-defined function. The boundary condition of the exit was defined as pressure exit with a relative pressure of 0. Non-slipping surface was used for the ground of the calculating domain and the surface of the cooling tower, and the side and symmetric boundary conditions were used for the top surfaces of the calculating domain, 3-D single precision discrete solver was used in numerical calculation. Due to the flow field where the cooling tower located was unsteady constant and the condition of turbulence flow was complex, the complicated flow field of cooling tower can be better simulated by LES. Smagorinsky-Lilly model was used for sub-grid scale and the pressure-velocity coupling equation sets were solved by SIMPLEX format which has good convergence and is suitable for LES calculation with small time step (Ke *et al*. 2015). Standard format was used for the discrete pressure item, Bounded Central Differencing format was used for dynamic discrete and second order

(a) working condition 1   (b) working condition 2   (c) working condition 3   (d) working condition 4
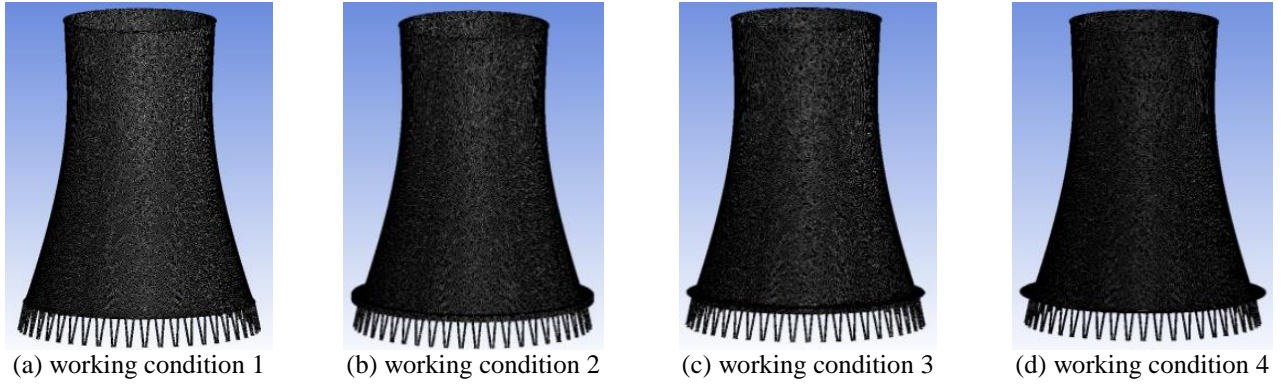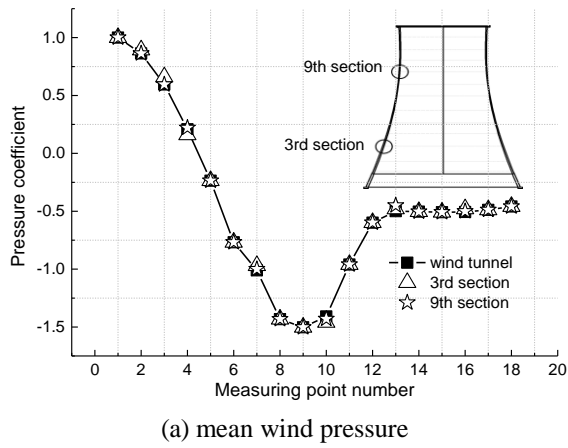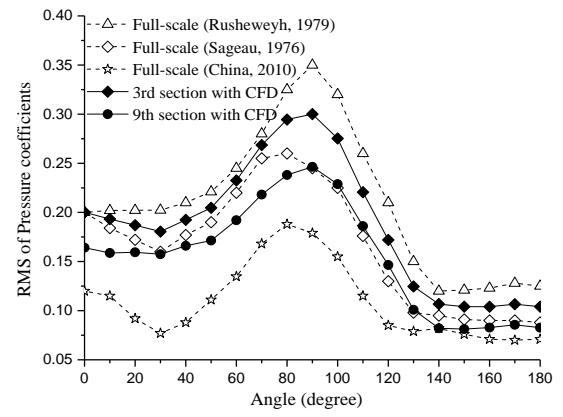
Fig. 6 The grid diagram of add different wind deflectors measures of cooling tower

(a) mean wind pressure

(b) fluctuating wind pressure

Fig. 7 Compared the wind pressure of CFD numerical simulation with field measurement and wind tunnel test

implicit differential equation was used for transient equation. The residual difference of calculation of control equations was 1×10^{-6} which was calculated by the model height and the average wind velocity at the model height with a time step of 0.001s.

3 Data analysis

3.1 Data processing method of wind tunnel test

The pressure on the surface of an object is generally expressed with the dimensionless pressure coefficient corresponding to the reference point, and the coefficient is determined by the following formula

$$C_{pi} = \frac{P_i - P_{+\infty}}{P_0 - P_{+\infty}} \qquad (1)$$

In the formula, P_i is the pressure at the measuring point i; P_0 and $P_{+\infty}$ are the total pressure and static pressure at the reference heights during the test, respectively. The pressure symbol is defined as follows: the surface pressure is positive when it is inward relative to the cooling tower walls and negative when it is outward.

The maximum instantaneous wind pressure coefficient on the surface of a building can be expressed as the sum of the mean and fluctuating values

$$C_{pext} = C_{pmean} \pm g C_{prms} \qquad (2)$$

where C_{pext}, C_{pmean} and C_{prms} is the extreme, mean and root mean square of fluctuating pressure coefficient, respectively. Its value is the ratio between the surface pressure and reference pressure and g is the peak factor. Whether the right of the equation takes the plus or minus symbol can determine whether a positive or negative pressure extreme coefficient is obtained.

In the Gaussian process hypothesis, Davenport (Davenport 1967) proposed a peak factor calculation method, which is as follows

$$g = \sqrt{2\ln(vT)} + \frac{0.57}{\sqrt{2\ln(vT)}} \qquad (3)$$

where v stands for the number of times that data can go through the mean per unit time; T stands for the length of time calculated.

The overall drag coefficient of the tower C_D is used to represent the wind pressure that the tower body suffers in the downwind, which is calculated as

|(a) working condition 1|(b) working condition 2|(c) working condition 3|(d) working condition 4|
(1) The vortex distribution of section on Y=0m

(a) working condition 1   (b) working condition 2   (c) working condition 3   (d) working condition 4
(2) The vortex distribution of section on Z=65m

(a) working condition 1   (b) working condition 2   (c) working condition 3   (d) working condition 4
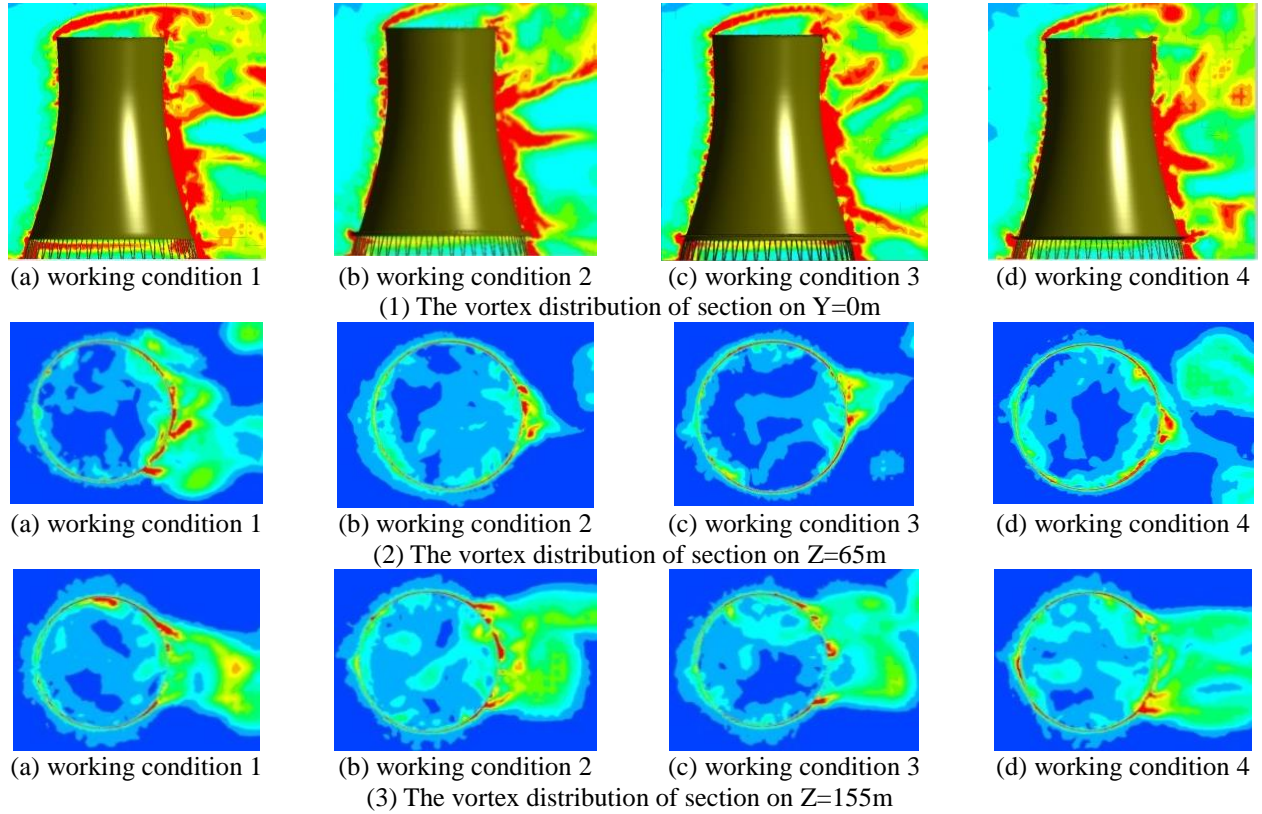(3) The vortex distribution of section on Z=155m

Fig. 8 The vorticity distribution of cooling towers with different deflectors on typical sections

$$C_D = \frac{\sum_{i=1}^{n} C_{pi} A_i \cos\theta_i}{A_T} \qquad (4)$$

where A_i is the pressure coverage area at the ith point; θ_i is the angle between the pressure at the ith measurement point and wind axis; and A_T is the area that the integral structure projects on to the direction of the wind axis.

3.2 Verify the effectiveness of CFD numerical simulation

In order to verify the correction of simulation method for cooling tower, Fig. 7 shows the mean and fluctuating wind pressures of typical sections on the cooling tower without wind deflector, which also compared with the field measurements and wind tunnel testing distribution curves.

The results show that the distribution of average wind pressure coefficients by the large eddy simulation is almost same as given by standard. The fluctuating wind pressure distribution curves for 3rd and 9th sections are among the measured curve at home and abroad, and the distribution trend in circumference are relatively close. We obtained the domestic and foreign field measurement, and wind pressure sensor height in the vicinity of 90 m, and found that the turbulence intensities are near to 0.110; however, the fluctuating wind pressure numerical test results are slightly different. This may be due to the cooling tower structure feature size and the topography, surrounding interference

etc. So taking into consideration that the fluctuating wind pressure distribution are closely related to the terrain of the measured tower, inflow turbulence and the surrounding disturbances, the fluctuating wind pressure distribution trend and values were obtained by large eddy simulation both in the envelope of the measured results, the comparison demonstrates that the simulating method of aerodynamic performance for cooling towers in this paper is accurate and steady. (Holmes 2002, VGB-Guideline 2005, Ramakrishnan and Arumugam 2012, Zhao *et al.* 2014, Ruscheweyh 1975, Sageau and Hamonou 1979).

4 The result analysis

4.1 Mean wind pressures

Fig. 8 gives the vortex distribution diagram of three typical sections for cooling towers with different wind deflectors, it could be found that the difference of vorticity distribution with different wind deflectors in the throat section was small, but on the lower section, it is evident from the figure that obvious vorticity increment region appeared on the leeward face, the range of vorticity induced by the wind deflectors was significantly larger than the wake vortex region of the tower without wind deflector.

Fig. 9 shows the distribution curves of the average pressure coefficients at four typical cross sections on the tower surface. Fig. 10 presents the meridional pressure coefficient distribution curves when the tower is at the four
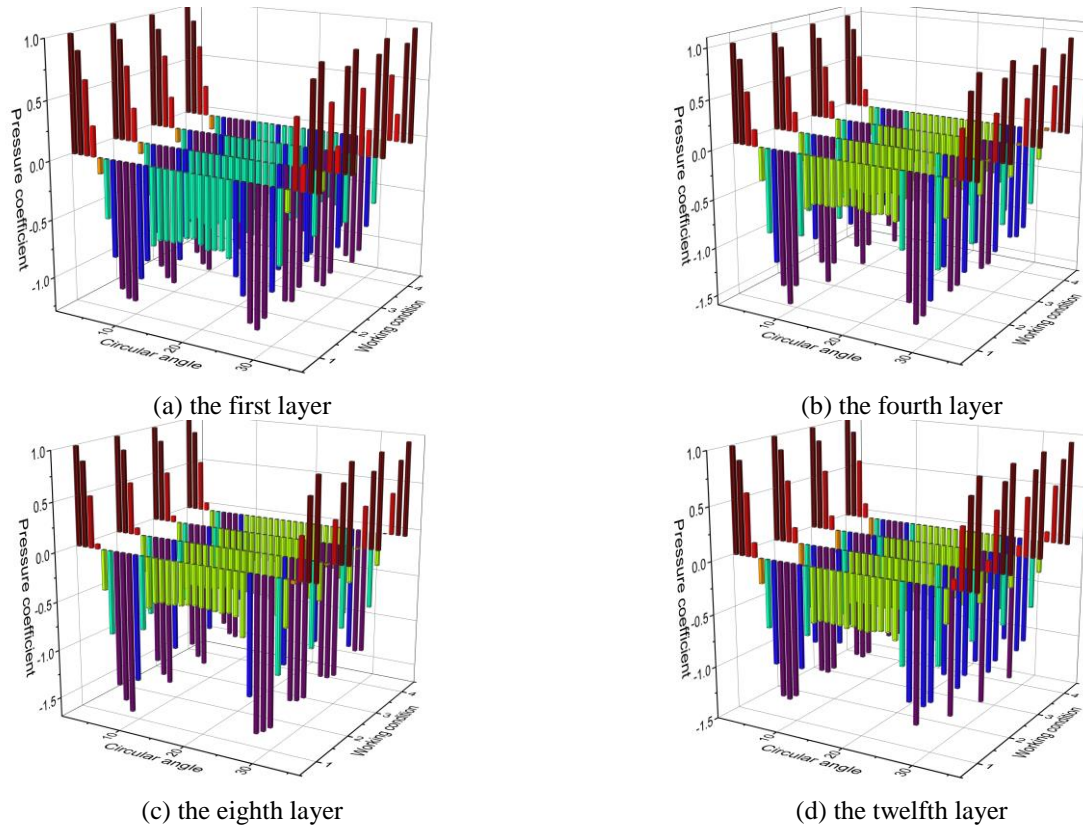
(a) the first layer

(b) the fourth layer

(c) the eighth layer

(d) the twelfth layer

Fig. 9 Comparison of pressure coefficient at measuring points of typical layers

typical angles of 0°, 70°, 120° and 180°. The comparison of the two figures reveals as follows:

i. The impacts of different wind deflecting devices on the pressure coefficient of the windward side of the tower are small, but the impacts on the pressure coefficient of the side and the leeward side of the tower are significant; the addition of the air deflecting devices does not make a significant difference between the pressure coefficients of the lower part of the cooling tower at 0° and 70° in the meridional direction, but increases the pressure coefficients at both 120° and 180° in the meridional directions, and the most obvious effect occurs at 180° in the meridional direction with an increase of 16.3%;

ii. Application of a wind deflecting device can effectively reduce the pressure coefficients of the central region of the tower at 70° in the meridional direction, and under working condition 2 the reduction can be about 6.6%;

iii. Different wind deflecting devices only significantly affect the pressure coefficients of the upper region of the tower at 180° in the meridional direction, but relatively little in other areas. The analysis showed that adding the wind deflecting devices best improved the mean wind pressure of the tower surface at 70° in the meridional direction, and can effectively reduce the pressure coefficients of the negative pressure extreme areas.

4.2 Fluctuating wind pressure

The root mean square of the pressure coefficient is an important indicator used to measure the energy level of the fluctuating pressure. Fig. 11 shows the change contour of root mean square of the fluctuating pressure on the surface of the cooling towers under four working conditions along as the circumferential angle and the meridional height change.

As can be seen from Fig. 11, the distribution pattern of root mean square of fluctuating wind pressure is very different from the average pressure results. The root mean square of the fluctuating wind pressure under working condition 1 is evenly distributed along the meridional and circumferential directions and with the increase of the circumferential angle, the pulsating pressure decreases and then increases before it finally reduces again and gradually stabilizes. The RMS value of the fluctuating wind pressure reaches its peak at between 80° ~ 100° on both sides of the tower; as the meridional height increases, the fluctuating wind pressure value on the windward side increases, but stays relatively stable on the leeward side.

The RMS of fluctuating wind pressure under all four working conditions have similar variation pattern, and the values of the fluctuating wind pressure at the measuring point on the leeward side are closer; as the side of tower is the separation zone, fluctuating wind pressure coefficients significantly increase, but the addition of the wind deflector can effectively reduce the pulsating pressure; different wind
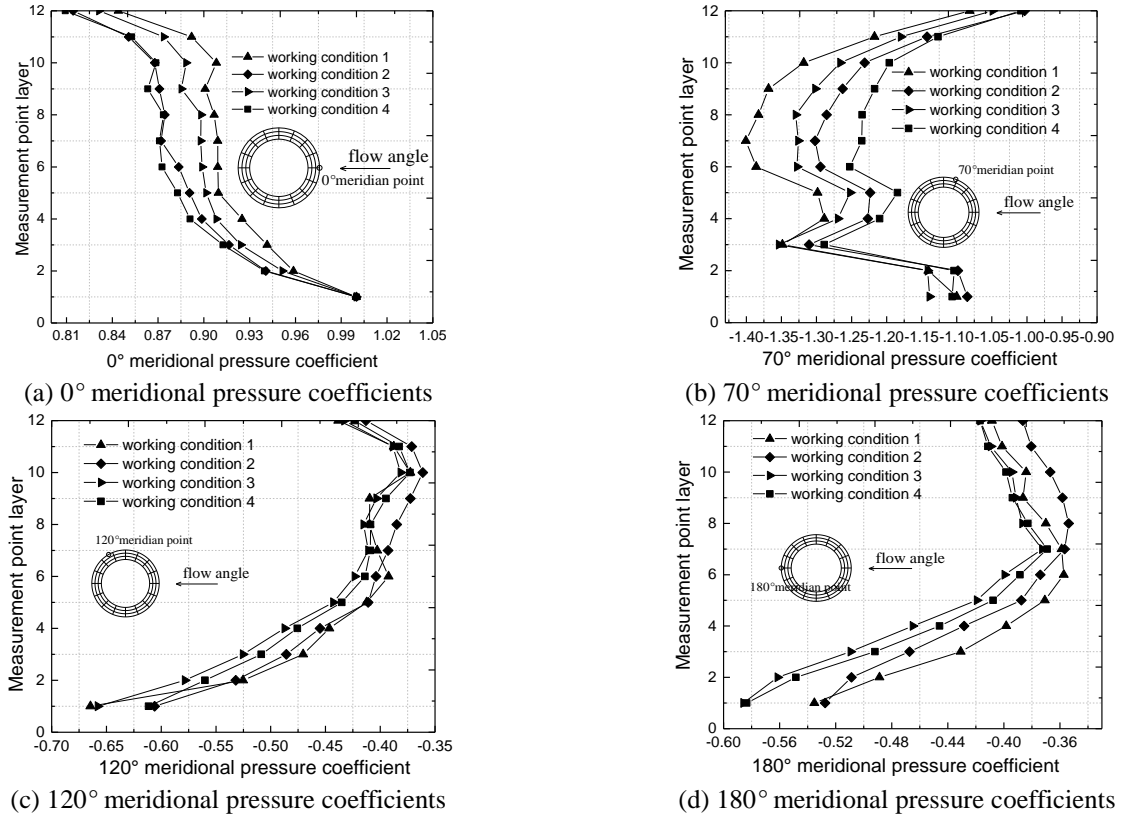
(a) 0° meridional pressure coefficients

(b) 70° meridional pressure coefficients

(c) 120° meridional pressure coefficients

(d) 180° meridional pressure coefficients

Fig. 10 The pressure coefficients under different meridian angles with different wind deflectors

(a) Height 34 m (inlet position)

(b) Height 150 m (throat position)

(c) Height 196 m (top outlet position)
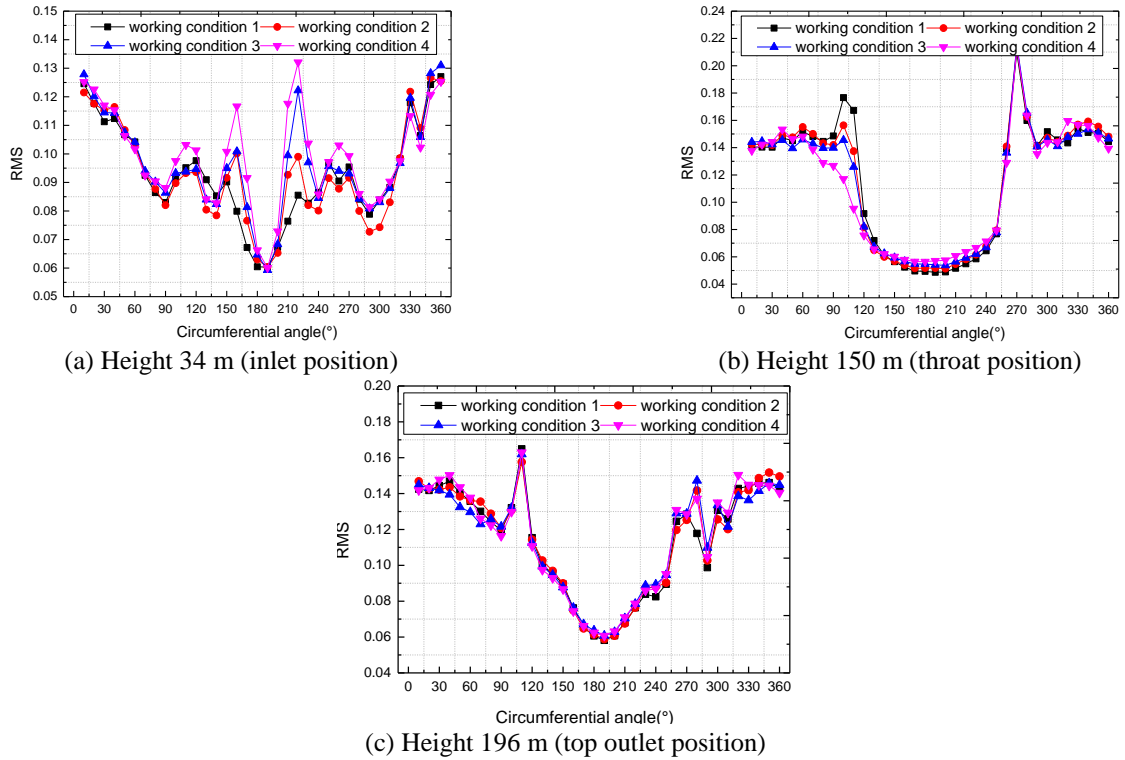
Fig. 11 The pulsating wind pressure distribution at typical high under four working conditions

Table 2 The average value of the peak factor in different regions under four working conditions

	regions	Condition 1	Condition 3	Condition 3	Condition 4
	Layers 1-4	3.33	3.34	3.34	3.34
A	Layers 5-8	3.29	3.30	3.30	3.31
	Layers 9-12	3.24	3.26	3.26	3.25
	Mean	3.29	3.30	3.30	3.30
	Layers 1-4	3.43	3.43	3.42	3.41
B	Layers 5-8	3.41	3.42	3.42	3.43
	Layers 9-1	3.40	3.41	3.410	3.42
	Mean	3.41	3.42	3.48	3.42
	Layers 1-4	3.51	3.46	3.46	3.44
C	Layers 5-8	3.56	3.54	3.54	3.52
	Layers 9-12	3.20	3.51	3.49	3.48
	Mean	3.52	3.50	3.50	3.48

deflectors are effective to a certain extent in reducing the RMS of the fluctuating wind pressure on the upper-middle part of the windward side of the tower, and the most significant effect occurs under working condition 4.

4.3 Peak factor

Ke and Ge (2015) studied the fluctuating wind pressure of cooling towers without wind deflectors and concluded that the values of peak factors are generally between 3.0 to 5.0. In order to study the impact of different wind deflectors on the values of the peak factor of fluctuating wind pressure on cooling towers, this study adopted Davenport peak factor method and calculated the peak factor of each measuring point under the respective working conditions based on the Gaussian process hypothesis. The time distance of wind pressure T was defined as 600s, and finally the reference values of peak factors of the cooling towers under each working condition were provided. Fig. 12 shows the distribution range of the peak factors at all measuring points on the surface of the cooling tower with different wind deflectors.

The comparison in the figure indicates that 1) the pattern of change in the peak factors of all the measuring points in the circumferential direction is the same under different working conditions, and the values of the peak factors of the windward and leeward sides are significantly different. The peak factor of the leeward side is significantly greater than that of other areas in the circumferential direction, with the maximum value reaching 3.6; 2) due to the interference from the aerodynamic measures, the peak factor of much of the lower part on the windward side is greater than the values at other heights. With the increase of height along the meridional direction, the peak factor shows a gradual downward trend. However, the distribution of the peak factors is less concentrated with great variations in value on the leeward side which is affected by both the wind deflector and the vortex shedding; 3) different wind deflectors can significantly reduce the peak factor of the lower part of the cooling tower on its leeward side.

In order to facilitate designers to select more reasonable peak factors, Table 2 lists the average values of peak factor of different areas on the surface of cooling towers when installed with different air reflectors.

Fig. 13 also presents sections along the circumferential direction on the cooling tower and the corresponding values of their peak factor.

4.4 Correlation coefficient of fluctuating wind pressure

The fluctuant pressures are related to organized large-scale vortex, which is expressed as a stronger correlation for the wind pressure space. The correlation coefficient is an important index for the inspection of the correlation between any two measuring points, and capable of reflecting the structure for the spatial flow field on the surface of the cooling tower and the transmission method thereof. We took the absolute value of the correlation coefficient, and only the correlations between the strengths of measuring points are analysed.

Fig. 14 shows the distribution diagram of correlation coefficients for measuring points on the typical sections (3rd and 9th layers). For the different areas in the circular section, the attenuation for the measuring point wind pressure of the windward side is very fast, in which all the measuring points belong to weak (relatively weak) correlation, and the wind pressure signals in the area are basically featured with Gaussian characteristics (Ke *et al.* 2015). In the negative extreme value area and the separation area, the cross-correlation is stronger. And more than two-thirds of the measuring points are outside the weak correlation area, the correlation between the negative extreme value and the separation point is strong, and the correlation of the protected side is gradually attenuated with the increased of circular angle.

4.5 wind pressure extremes

The existing cooling tower design specifications and research findings do not touch upon the distribution of wind
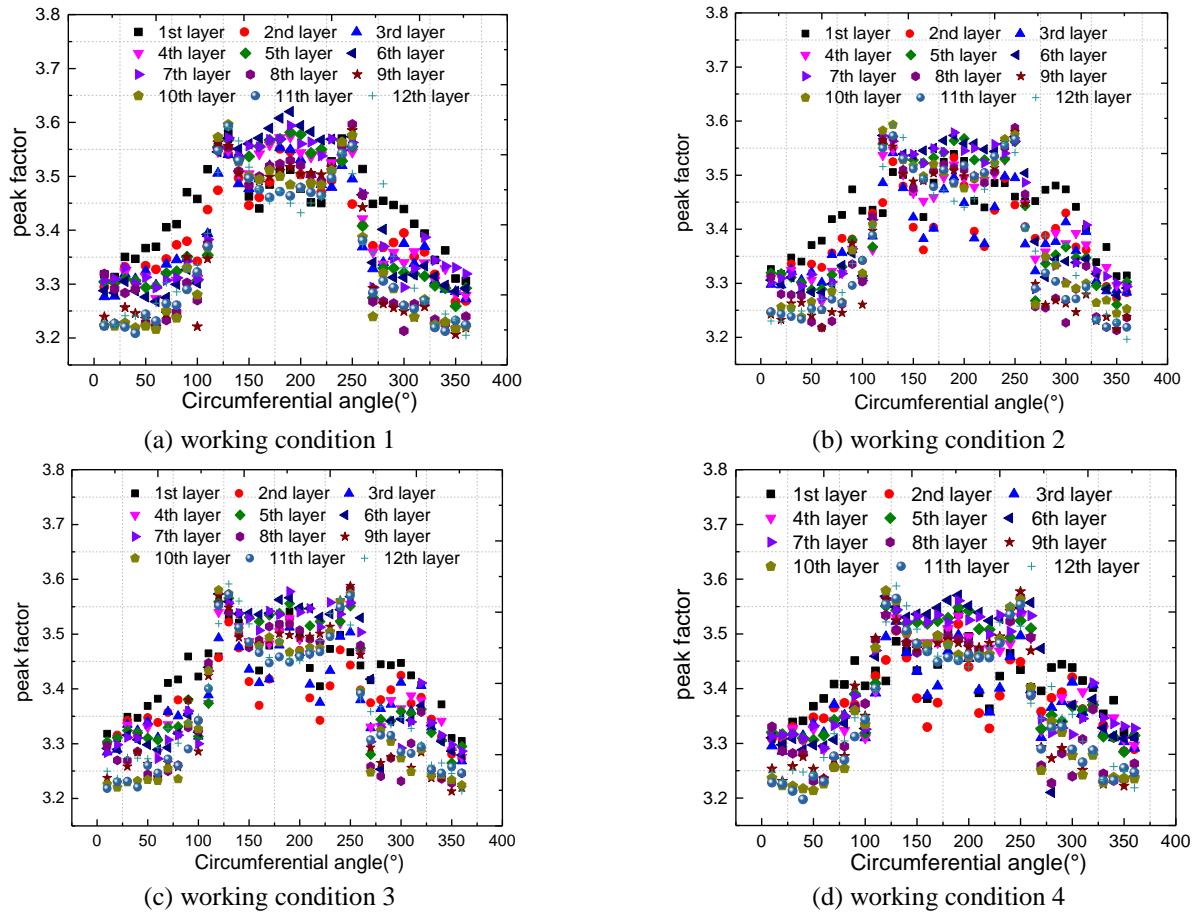
Fig. 12 The peak factors for cooling towers with different wind deflectors under four working conditions
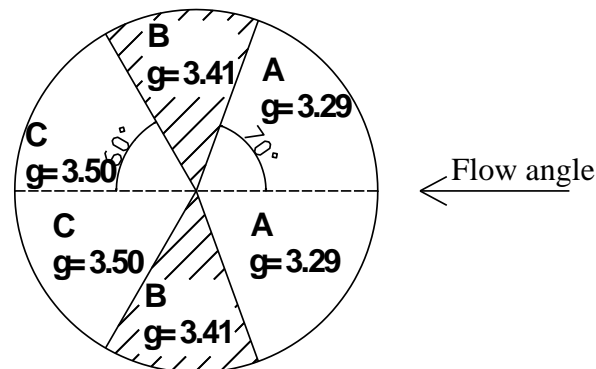

Fig. 13 Reference value of peak factor in sections in the circumferential direction

pressure extremes on the surface of cooling towers installed with different wind deflectors (Holmes 2002, Zhang *et al.* 2011). Figs. 15 and 16 present the contour of the maximum value and the minimum value of the wind pressure coefficient on the surface of cooling towers under four working conditions.

The comparison reveals that under four kinds of conditions the maximum pressure coefficient occurred at 0° angle position in the windward side of the tower, increasing the aerodynamic measures has less effect for the upper part of the tower pressure coefficient maximum value, but the impact on the lower-middle part of the tower is obvious; different wind deflectors can effectively reduce the maximum wind pressure coefficient value on the windward side, in which the effect of working conditions four and two are the most obvious; different wind deflectors can be effective in reducing the minimal pressure coefficient in the negative extreme value area on the upper portion of the tower, working conditions three has the best effect; in the region of negative pressure extremes, the maximum wind pressure coefficient significantly decreases due to reduced contribution of pulsating pressure in the lower part of the
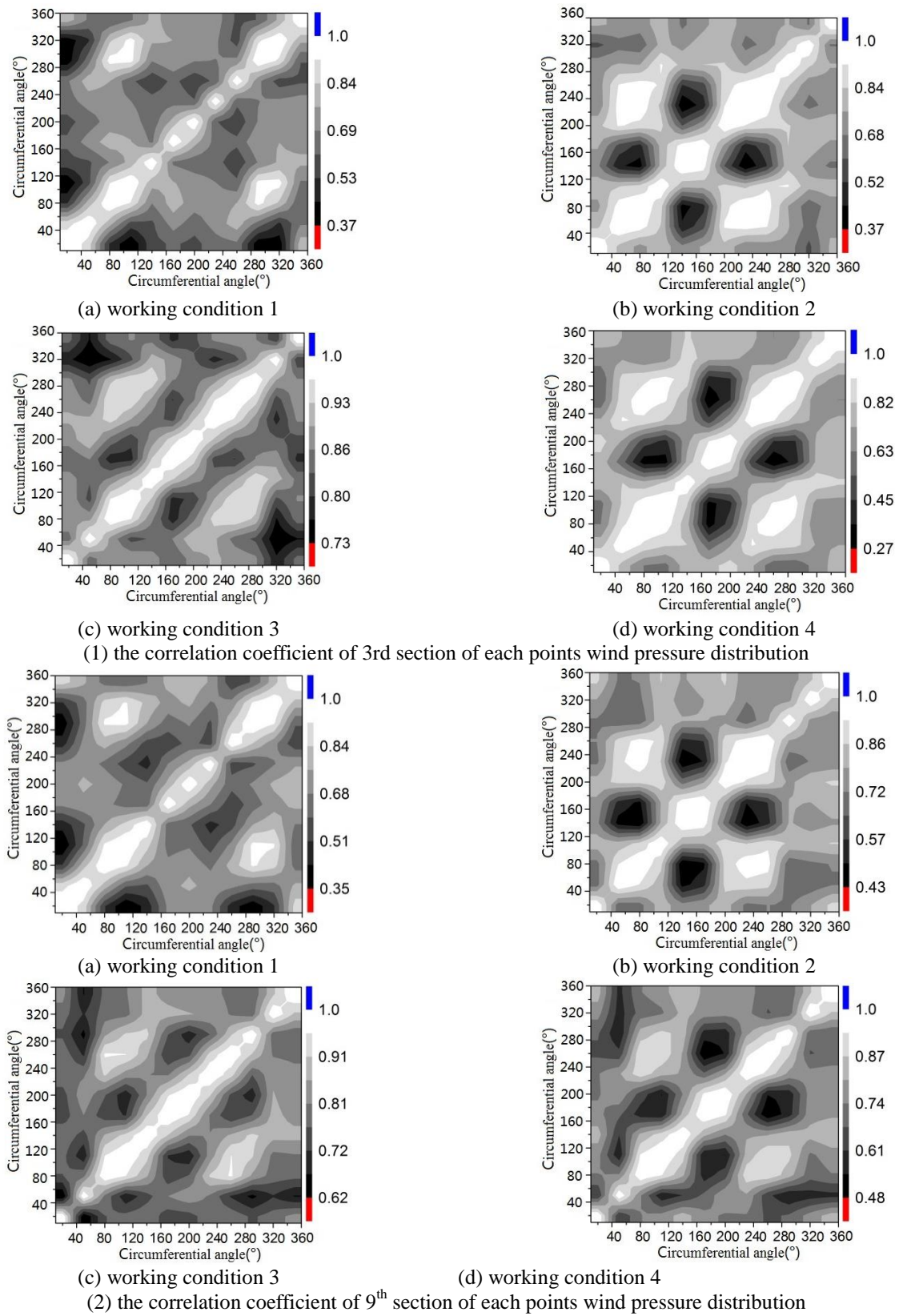
(a) working condition 1　　　　　　　　　　(b) working condition 2

(c) working condition 3　　　　　　　　　　(d) working condition 4

(1) the correlation coefficient of 3rd section of each points wind pressure distribution

(a) working condition 1　　　　　　　　　　(b) working condition 2

(c) working condition 3　　　　　　　　　　(d) working condition 4

(2) the correlation coefficient of 9th section of each points wind pressure distribution

Fig. 14 The distribution diagram of correlation coefficients for measuring points on the typical sections

(a) working condition 1

(b) working condition 2

(c) working condition 3

(d) working condition 4
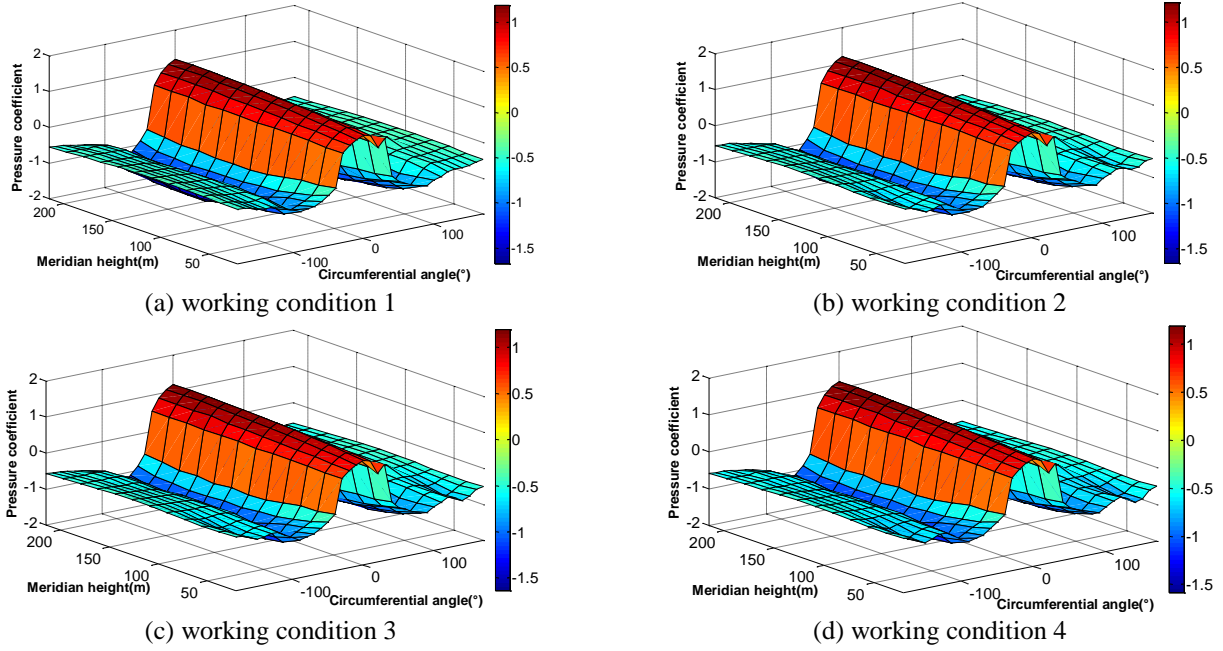
Fig. 15 Contour of maximum value of the surface pressure coefficient under different working conditions

(a) working condition 1

(b) working condition 2
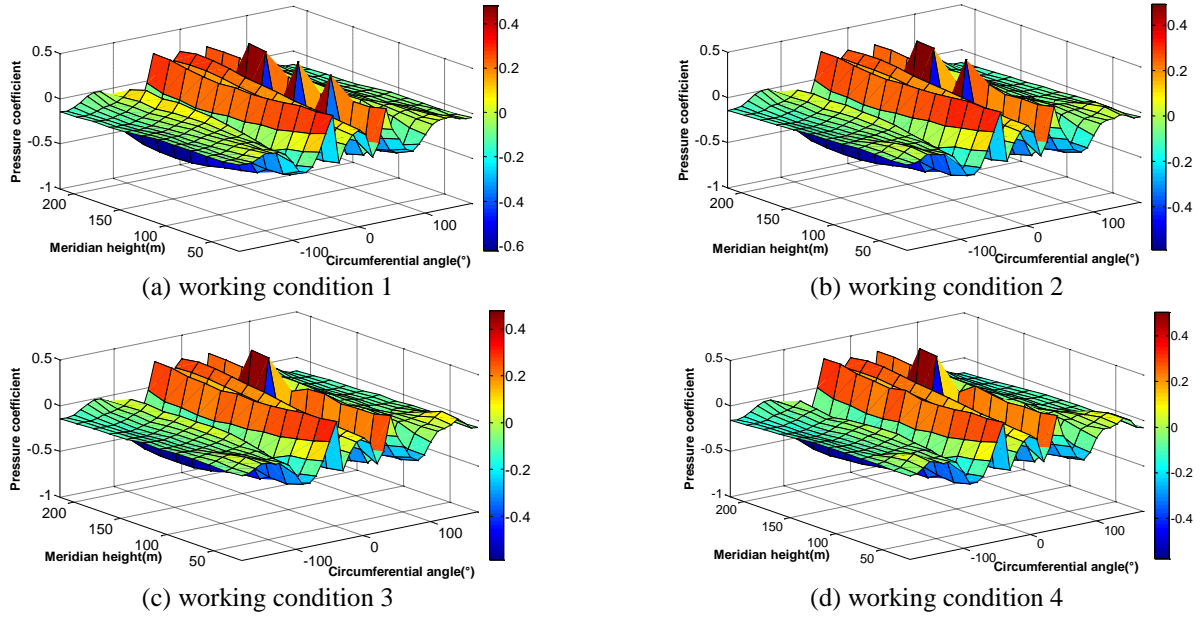
(c) working condition 3

(d) working condition 4

Fig. 16 contour of minimum value of surface pressure coefficient under different working conditions

cylindrical tower under working condition four, while in the area on the leeward side, due to the vortex shedding and wake, the negative extreme value distribution becomes disorderly.

Considering the average wind pressure coefficients under four working conditions, and the impact of fluctuating wind pressure, based on the principle of least squares method, the fitting was conducted using Fourier series expansion on coefficients of the shape extreme value distribution curve

$$\mu_P(\theta) = \sum_{k=0}^{m} a_k \cos k\theta \pm \sum_{k=0}^{m} b_k \cos k\theta \qquad (5)$$

It is found when $m \geq 7$ it is possible to achieve good fitting effect. Table 3 shows in the four working conditions when $m = 7$ the values of parameters a_k and b_k in the fitted formula values. Fig. 17 shows the comparison curve of calculation results of fitting formula under four working conditions and the experimental data.

Table 3 List of values of the fitting parameters a_k and b_k

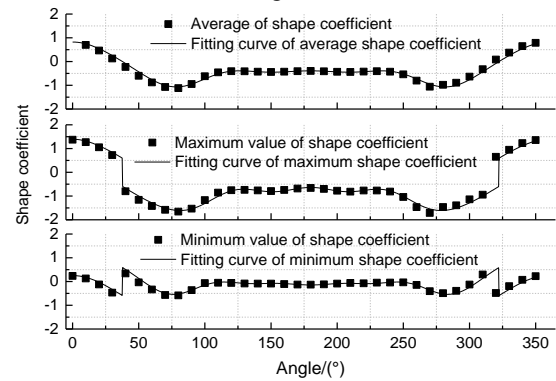| Condition	Condition 1	Condition 2	Condition3	Condition 4
a_0	-0.3594	-0.3570	-0.3602	-0.3504
a_1	0.3091	0.3309	0.3337	0.3452
a_2	0.6009	0.5877	0.5704	0.5518
a_3	0.3244	0.3254	0.3201	0.3209
a_4	-0.0475	-0.0375	-0.0318	-0.0175
a_5	-0.0660	-0.0702	-0.0703	-0.0718
a_6	0.04259	0.0413	0.0371	0.03114
a_7	0.0113	0.0108	0.0116	0.0123
b_0	0.4652	0.4760	0.4760	0.4754
b_1	0.1693	0.1587	0.1587	0.1413
b_2	-0.0765	-0.0550	-0.0550	-0.0508
b_3	0.0123	0.0036	0.0036	0.0045
b_4	0.0346	0.0276	0.0276	0.0239
b_5	-0.0255	-0.0223	-0.0223	-0.0159
b_6	-0.0272	-0.0386	-0.0386	-0.0400
b_7	0.0278	0.0339	0.0339	0.0320
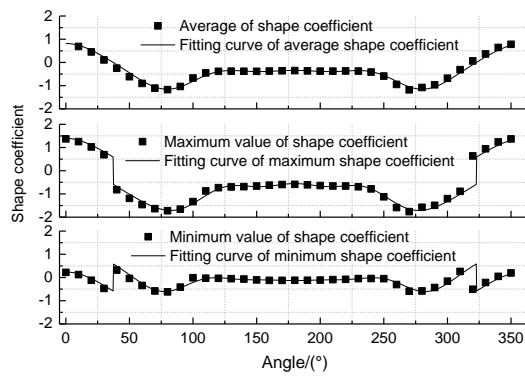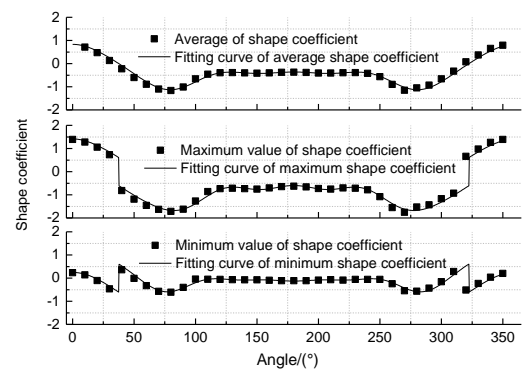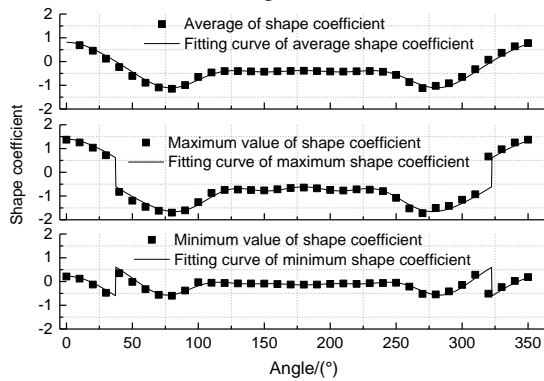
(a) working condition 1 (b) working condition 2 (c) working condition 3 (d) working condition 4

Fig. 17 Comparison between the raw data and the fit data

4.6 drag coefficient

Fig. 18 shows the comparison of drag coefficients at typical height of the cooling towers with different wind deflectors. As can be seen from the figure, all the global drag coefficients of the four conditions appear the similar change rule, the wind deflectors have significant effect on the increase in drag coefficient of each layer of the lower middle parts of the tower, especially in the windward of cooling tower. The drag coefficient under condition 4 reached its maximum value, which was approximately 18% greater than the drag coefficient under condition 1.
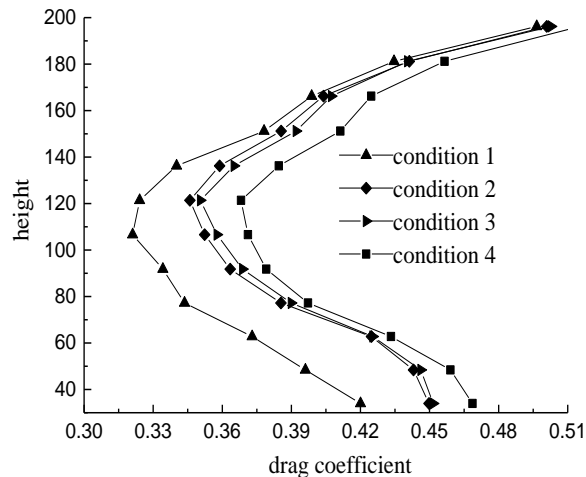
S.T. Ke, P. Zhu and Y.J. Ge

Fig. 18 The drag coefficients at each layer under different calculating conditions

5 Conclusions

Based on the pressure measurement experiment and numerical simulation, the pattern of impact of different wind deflectors on the aerodynamic parameters was revealed. The following major conclusions were made.

1) Different wind deflectors can be effective in reducing the mean wind pressure in the centre of the tower cylinder at 70° meridional direction. The most significant effect was observed under condition 2 with a reduction of about 6.6%. And add wind deflectors could effectively reduce the root mean square of the fluctuating wind on leeward side, with working condition 4 showing the most significant effect.

2) Different wind deflectors could all significantly reduce the peak factor of the lower part on the leeward side of the tower. The peak factor on leeward side was significantly greater than that of the other circumferential areas, with the maximum value reaching 3.6. As the meridional altitude increased, the peak factors showed a gradual downward trend. At the end of the paper, a figure showing the circumferential distribution of the peak factor values of the cooling towers with different wind deflectors.

3) Under four kinds of working conditions, the maximum values of wind pressure coefficient all occurred in the windward side of the tower at 0° angle position. The effect of an increase in aerodynamic measures on the maximum value of the pressure coefficient at the upper part of the tower was negligible, but significant on the lower part of the tower. All different wind deflectors reduced the maximum value of the windward side and negative pressure extreme regions, and the most obvious effect occurred under working conditions 2 and 4. The final Formula (5) provides a fitting formula of the pressure extremes on the surface of extra-large cooling towers installed with different wind deflectors and no wind deflector.

4) The wind deflectors have obvious influence on the correlations of measured points, such as working condition 2 and 4 especially increase the correlation in the negative extreme value area, but weaken correlation in the windward and leeward sides. The wind deflectors have significant effect on the increase in drag coefficient of each layer of the

lower middle parts of the tower, and the drag coefficient under condition 4 reached its maximum value, which was approximately 18% greater than the drag coefficient under condition 1.

In summary, it was demonstrated that the aerodynamic effects of different wind deflectors on large cooling towers are significant, which was suggested to be taken into account for wind tunnel tests and wind-resistant design of such structures.

References

Armitt, J. (1980), "Wind loading on cooling towers", *J. Struct. Div.*, **106**(3), 623-641.

Bartoli, G., Borri, C., Hoeffer, R. and Orlando, M. (1997), "Wind induced pressures and interference effects on a group of cooling towers in a power plant arrangement", *Proceedings of the 2nd European and African Conference on Wind Engineering*, Genoa, Italy, Padua, SGE.

Busch, D., Harte, R., Kratzig, W.B. and Montag, U. (2002), "New natural draught cooling tower of 200 m height", *Eng. Struct.*, **24**(12), 1509-1521. https://doi.org/10.1016/S0141-0296(02)00082-2.

Davenport, A.G. (1967), "Gust loading factors", *J. Struct. Div. – ASCE*, **93**(3), 11-34.

Goudarzi, M.A. and Sabbagh-Yazdi, S.R. (2008), "Modeling wind ribs effects for numerical simulation external pressure load on a cooling tower of Kazerun power plant-Iran", *Wind Struct.*, **11**(6), 479-496. http://dx.doi.org/10.12989/was.2008.11.6.479.

Goudarzi, M.A. and Sabbagh-Yazdi, S.R. (2008), "Modeling wind ribs effects for numerical simulation external pressure load on a cooling tower of KAZERUN power plant-IRAN", *Wind Struct.*,

11(6), 479-496. http://dx.doi.org/10.12989/was.2008.11.6.479.

Harte, R. and Wittek, U. (2009), "Recent developments of cooling tower design", *Proceedings of the IASS Symposium*, Valencia, Spain, Sept.-Oct.

Holmes, J.D. (1992), "Optimized peak load distributions", *J. Wind Eng. Ind. Aerod.*, **41**(1), 267-276.

Holmes, J.D. (2002), "Effective static load distributions in wind engineering", *J. Wind Eng. Ind. Aerod.*, **90**(2), 91-109. https://doi.org/10.1016/S0167-6105(01)00164-7.

Isyumov, N. and Abu-Sitta, S.H. (1972), "Approaches to the design of hyperbolic cooling towers against the dynamic action of wind and earthquakes", *Bull. Int. Assoc. Shell Struct.*, **48**, 3-22.

Ke, S.T., Liang, J., Zhao, L. and Ge, Y.J. (2015), "Influence of ventilation rate on the aerodynamic interference for two IDCTs by CFD", *Wind Struct.*, **20**(3), 449-468. http://dx.doi.org/10.12989/was.2015.20.3.449.

Ke, S.T., Ge, Y.J., Zhao, L. and Tamura, Y. (2012), "A new methodology for analysis of equivalent static wind loads on super-large cooling towers", *J. Wind Eng. Ind. Aerod.*, **111**(3), 30-39. https://doi.org/10.1016/j.jweia.2012.08.001.

Ke, S.T., Ge, Y.J., Zhao, L. and Tamura, Y. (2013), "Wind-induced responses characteristics on super-large cooling towers", *J. Central South Univ. Technol.*, **20**(11), 3216-3227.

Ke, S.T. and Ge, Y.J. (2014), "The influence of self-excited forces on wind loads and wind effects for super-large cooling towers", *J. Wind Eng. Ind. Aerod.*, **132**, 125-135. https://doi.org/10.1016/j.jweia.2014.07.003.

Ke, S.T. and Ge, Y.J. (2015), "Extreme wind pressures and non-Gaussian characteristics for super-large hyperbolic cooling towers considering aero-elastic effect", *J. Eng. Mech.*, **141**(7), 04015010. https://doi.org/10.1061/(ASCE)EM.1943-7889.0000922

Niemann, H.J. and Kopper, H.D. (1998), "Influence of adjacent buildings on wind effects on cooling towers", *Eng. Struct.*, **20**(10), 874-880.

Qiao, Q., Guo, Z. and Wang, R. (2011), "Wind Tunnel Experimental Study on Effect of Nuclear Power Plant Cooling Tower on Radioactive Plume Dispersion", Bioinformatics and Biomedical Engineering,(iCBBE), *Proceedings of the 5th International Conference on. IEEE*.

Ramakrishnan, R. and Arumugam, R. (2012), "Optimization of operating parameters and performance evaluation of forced draft cooling tower using response surface methodology (RSM) and artificial neural network (ANN)", *J. Mech. Sci. Technol.*, **26**(5), 1643-1650.

Ruscheweyh, H. (1975), "Wind loadings on the television tower, Hamburg, Germany", *J. Ind. Aerod.*, **1**, 315-333. https://doi.org/10.1016/0167-6105(75)90026-4.

Sageau, J.F. and Hamonou, M. (1979), "Application of data acquisition system for on site measurements of wind effects on structures",*Von Karman Inst for Fluid Dyn Data Acquisition Systems & Data Analysis in Fluid Dyn 26 P. In Von Karman Inst. for Fluid Dyn. Data Acquisition Systems and Data Analysis in Fluid Dyn.*, SEE N80-12354 03-34.

Sun, T.F. and Gu, Z.F. (1992), "Full-scale measurement and wind-tunnel testing of wind loading on two neighboring cooling towers", *J. Wind Eng. Ind. Aerod.*, 4**3**(1-3), 2213-2224. https://doi.org/10.1016/0167-6105(92)90660-3.

Sun, T.F. and Gu, Z.F. (1995), "Interference between wind loading on group of structures", *J. Wind Eng. Ind. Aerod.*, **54**(55), 213-225. https://doi.org/10.1016/0167-6105(94)00051-E.

VGB-Guideline (2005), "Structural design of cooling tower-technical guideline for the structural design, computation and execution of cooling towers", Standard Essen: BTR Bautechnik bei Kühltürmen.

Zhang, J.F., Ge, Y.J. and Zhao, L. (2011), "Effect of latitude wind

pressure distribution on the load effects of hyperboloidal cooling tower shell", *Proceedings of the 13th International Conference on Wind Engineering*. Amsterdam, Netherlands.

Zhao, L., Chen, X., Ke, S.T. and Ge, Y.J. (2014), "Aerodynamic and aero-elastic performances of super-large cooling towers", *Wind Struct.*, **19**(4), 443-465. http://dx.doi.org/10.12989/was.2014.19.4.443

Zhao, L., Chen, X. and Ge, Y. (2016), "Investigations of adverse wind loads on a large cooling tower for the six-tower combination", *Appl. Therm. Eng.*, **105**, 988-999. https://doi.org/10.1016/j.applthermaleng.2016.02.038.

FR